ADVANCED INTELLIGENT SYSTEMS
Open Access
www.advintellsyst.com

Worm-Inspired Soft Robots Enable Adaptable Pipeline and Tunnel Inspection

Xiaomin Liu, Maozheng Song, Yuhui Fang, Yunwei Zhao, and Changyong Cao**

The inspection, maintenance, and repair of pipeline and tunnel infrastructure have motivated the increasing research in the development of suitable robots with high flexibility, good adaptability, and large load capacity. Herein, a worm-inspired soft robot that is capable of operating and performing a variety of tasks in a complicated pipeline/tunnel environment is reported. The soft tubular robot consists of elongation pneumatic actuators (EPAs), radial expansion pneumatic actuators (REPAs), and a spatial bending pneumatic actuator (SBPA). A series of experiments are performed to demonstrate the capability of the soft robot to crawl robustly under different pipeline conditions, including varying diameter, different cross-sectional shapes, and wet or oil-covered internal surfaces, and underwater environment. The soft robot can carry a load of more than 11 times of its own weight in a vertical pipeline. Equipped with a visualization unit, the soft robot can detect the internal conditions of the pipeline and cross the multi-branched pipeline as needed. The tubular soft robot provides a useful tool for the inspection, cleaning, and maintenance of pipelines and tunnels.

1. Introduction

Pipelines are commonly used for the transport of water, oils, and gases in industry. The need to inspect the pipelines for infrastructure maintenance and repair work has attracted much attention in developing suitable robotics for a variety of tasks, in particular in dangerous situations.[1] Most of previously developed robots are built with rigid materials/components, which may induce possible damage of the pipe surfaces due to concentrated stress or impact in operation. Usually, these rigid robots are designed for a specific pipeline, which limit the capability to be used for different pipe sizes, and complex shaped cross sections or multibranches in a nonuniform pipeline network.[2–4] Thus, it is necessary to invent a compliant, user-friendly robotics for safe interactions with people and environment. In this regard, soft robots composed of soft materials can supply a superior option for such applications[4,5] owing to their excellent flexibility and inherent compliance, as well as more degrees of freedom and adaptation to complicated and harsh environment.[6]

In recent years, researchers have designed several soft pipe-climbing robots for different applications.[7–10] For example, Seok et al.[10] proposed a soft mesh worm robot made of flexible mesh materials actuated by a NiTi coil spring. The entire mechanical structure can withstand significant external impacts. However, the sensitivity of the shape memory alloy (SMA) spring to the environmental temperature may result in instability and inefficiency issue in applications. Other kinds of soft material based actuators have also been used for designing soft robots such as ionic polymer metal composites[11] and dielectric elastomers (DEAs).[12] These soft robots use smart materials to generate deformation to move, cannot achieve a high moving speed. Yeh et al. developed a multilocomotion soft robot controlled by pulling and releasing of cables driven by two motors.[8,13] It can hop and crawl in vertical and horizontal pipes by using different actuation sequences and parameters. It is designed for a pipe with a specific diameter and is not compatible with a pipeline with variable diameters or other complicated tubes. Recently, some tubular robot driven by pneumatic or hydraulic pressure have demonstrated promise for pipeline applications.[14] Verma et al.[9] presented a soft tube-climbing robot built with buckling pneumatic actuators driven by a negative pressure. This soft robot has two clampers for anchoring and one linear actuator for moving. By expanding and contracting the actuators in sequence, the soft robot can move along a tube with varying diameter. The proposed buckling pneumatic actuators has only one degree-of-freedom (DOF), thus the soft robot cannot adjust the heading direction in a connected pipe network.

To augment the performance of soft robots, bending actuators have been proposed to mimic the inchworm's deformation of the soft body. For instance, Tang et al. designed and fabricated a soft robot with a soft bending actuator. Nevertheless, the classic

X. Liu, M. Song, Y. Zhao
School of Mechanical Engineering
Beihua University
Jilin 132013, China
E-mail: jluzyw@163.com, yw_zhao@beihua.edu.cn
Y. Fang, C. Cao
Laboratory for Soft Machines and Electronics
School of Packaging
Departments of Mechanical Engineering
Electrical and Computer Engineering
Michigan State University
East Lansing, MI 48824, USA
E-mail: ccao@egr.msu.edu
The ORCID identification number(s) for the author(s) of this article can be found under https://doi.org/10.1002/aisy.202100128.

DOI: 10.1002/aisy.202100128

pneumatic bending actuator can only bend in a 2D plane and the soft robot exhibits single DOF in motion.[15] Inspired by the extraordinary characteristics of inchworm locomotion, Boyu et al. developed a soft robot with multi-DOF extension module to adjust the heading direction in space and elongate its body, which greatly improved its practical applications in different tubular environments.[2] In this design, although the soft robot can simultaneously bend and elongate its body, the bending angle and elongation are coupled together so that it is hard to control the bending direction in operations.

In this work, we propose a new modular design of soft tubular robot capable of moving along a complex pipeline with varying diameter or multibranches. The soft robot consists of three major pneumatic actuators: elongation pneumatic actuator (EPA), radial expansion pneumatic actuator (REPA), and spatial bending pneumatic actuator (SBPA), which are soft and have high flexibility. The inner surface condition of the pipeline can be dry, wet, or oil-covered. The soft robot having multiple actuators or modules can be equipped with a steering module with more DOFs which can bend along arbitrary direction in a 3D space. The FEM simulations and experiments are performed to analyze the deformations of the soft actuators and the output force of each module to predict the motion performance and load capacity of the soft robot. This soft tubular robot has the merits of fast response, lightweight, low cost, robust actuation, and ease of fabrication. It is demonstrated that the new soft robot can be utilized in different applications such as removing obstacles, cleaning interior of pipelines, and detecting the defects of pipelines with various diameters and multiple branches, under complicated surface conditions (dry, wet, oil-covered, or underwater).

2. Design and Fabrication of the Worm-Inspired Soft Robot

2.1. Concept Design and Fabrication

Inspired by worm, we propose a new soft tubular robot made of multiple soft actuators using silicone rubber in a modular manner. The basic module of the soft robot consists of two REPAs and one EPA to crawl effectively in a pipeline. The two REPAs are used as feet (forefoot and the hindfoot) to adhere to the inner surface of a pipeline, while the EPA is used as the main body to propel it forward like a worm. The soft tubular robot has excellent flexibility and functionality and may be potentially used for performing inspection or delivery tasks safely in pipelines or tunnels under complex environment conditions.

As shown in **Figure 1**a, the inner space of the REPA is divided into four annular independent chambers by a diaphragm (3 mm thick), and the four chambers are connected by a unified pneumatic channel. The thickness of the sidewall of the REPA is 2 mm, and the upper and lower end surface wall is 4 mm. When a pneumatic pressure is applied onto the chamber, the REPA expands radially and uniformly. Similarly, the EPA has two connected chambers (2 mm wall thickness) along the axial direction so as to elongate its body when an air pressure is applied. In our design, both EPA and REPAs are equipped with central channels for accommodating the air tube and the pneumatic channels for actuation. To facilitate the assembly for soft robots, the ends of the EPA have bosses designed for connection with the REPAs. Four grooves are evenly embedded on the surface of REPAs as the drainage channels to reduce the motion resistance when the soft robots crawl in a pipeline filled with liquids or gases.

When actuated, the feet actuators of the soft robot expand radially to adhere onto the inner surface of the pipeline to get the needed support force, while the body actuators axially elongate to propel its motion. The adhesion force of the feet is controlled by the actuation pressure to ensure a firm attachment in the pipes or tunnels. The alternative actuation of the forefoot, hindfoot, and body in a programmable way can drive the motion of the soft robot. Therefore, the proposed tubular soft robot is capable of passing through the pipes with different kinds of pipes with variable radius or cross-sectional shapes.

The feet and body actuators of the worm-inspired soft robot can be pneumatically actuated in a programmable manner. To demonstrate the mobility of the soft robot, we investigate two kinds of gait sequences: single gait and cross-gait (**Figure 2**) through a program of controlling the solenoid valves and proportional valves. We build a finite element model (ABAQUS 6.14) to simulate the motion process under different conditions. The actuation state (Pressure On) or relaxing state (Pressure Off) for each actuator is switched by the air pressure in the corresponding actuator in a specific sequence.

As shown in Figure 2a, single gait mode involves six steps in a complete motion cycle in which the feet and the body are actuated alternatively: 1) step 1: both the forefoot and hindfoot are pneumatically actuated at (ON state) and the soft robot can adhere to the inner wall of the pipe; the body actuator is deflated at OFF state. 2) Step 2: the forefoot deflates (OFF) and hindfoot remains inflated (ON). 3) Step 3: the body actuator of the soft robot inflates (ON) and axially elongates to push the forefoot stride forward. 4) Step 4: the forefoot is actuated again to stick on the inner wall of the pipe. 5) Step 5: the hindfoot deflates to the OFF state to lift off from the inner wall of the pipe. 6) Step 6: The body actuator deflates and retracts to its original length (OFF). At this time, the robot completes one cycle of forward motion and the stride length Δl is equal to the axial elongation of the EPA under the air pressure. t_f and t_b are the inflation duration of the feet and the body of the soft robot; t_d is deflation duration of all actuators.

To increase the moving speed of the soft robot, we further investigate the cross-gait mode in which the inflation or deflation of the feet actuators synchronizes with the elongation of the body actuator (Figure 2a). One cross-gait cycle includes four steps: 1) step 1: the hindfoot is actuated (ON) to touch on the inner wall of the pipe; 2) step 2: the body actuator is actuated (ON) and elongates along axial direction. After half inflation ($t = t_b/2$), the forefoot is actuated to stick to the inner wall of the pipe; c) step 3: the hindfoot actuator deflates to detach from the inner wall of the pipe; d) step 4: the body actuator is deflated and retracted to the initial length, and then at $t = t_d/2$ the hindfoot expands and adheres to the inner wall of the pipe. It is noted that when the soft robot moves forward in a single gait mode, only one actuator changes its state in each step, which leads to better stability of the robot. Therefore, single gait is more suitable for carrying a loading, such as transporting or removing obstacles in pipelines. For the cross-gait, two or more actuators change their states

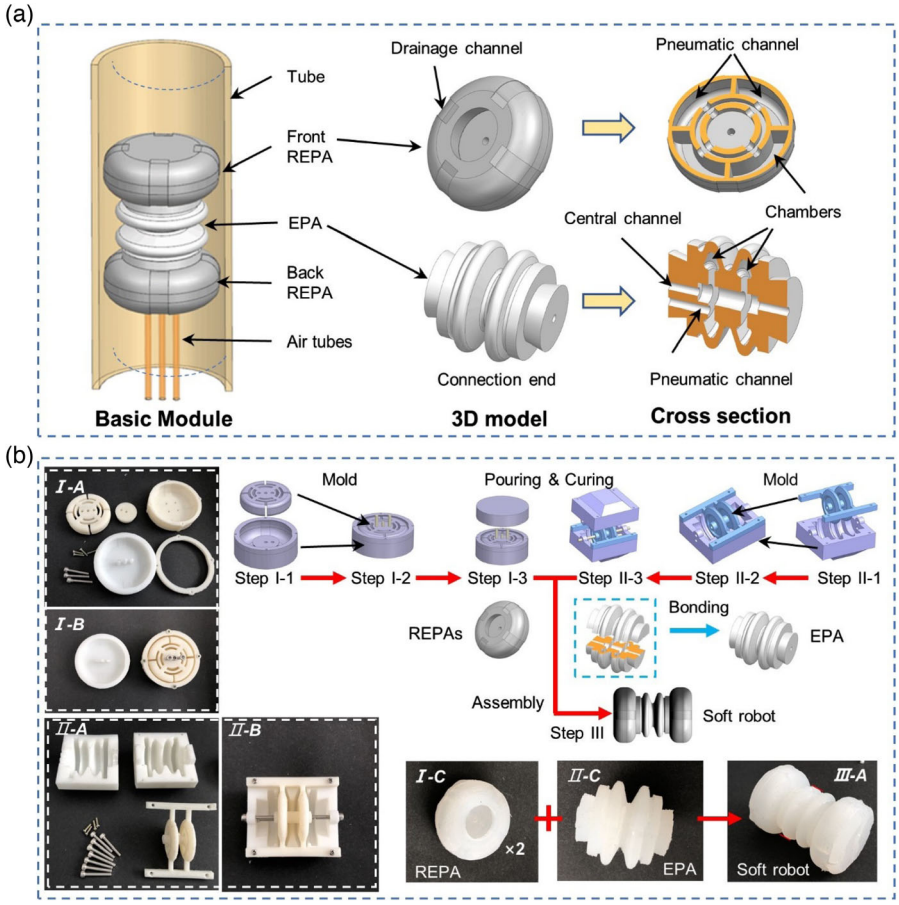

Figure 1. Concept design and fabrication of the worm-inspired soft robot. a) Schematic illustration of the basic module of the soft robot consists of an EPA as the main body and two REPAs fixed at two ends as its feet (i.e., forefoot and hindfoot). Both EPA and REPAs are equipped with central channels and pneumatic channels for accommodating air tubes and pneumatic actuation, respectively. There are four chambers in the REPA connected by a single pneumatic channel. The foot actuators of the robot expand radially when actuated by pneumatic pressure. The main body actuator elongates along the axial direction to drive the robot to move forward. b) Schematic illustration of the fabrication process for the basic module. The soft actuators are mold-casted with silicone rubber and the molds are printed by a 3D printer. Step I: Fabrication process of REPA. 3D printed molds for REPA (I-A and I-B), demolded sample of REPA (I-C). Step II: Fabrication process of the main body EPA. 3D printed molds for EPA (II-A and II-B). Demolded pieces and bonded EPA (II-C). Step III: Assembly of the basic module of the soft robot with forefoot, main body and hindfoot bonded together (III-A).

simultaneously, which results in a faster motion speed. In practice, these two gaits can be adopted on-demand. For example, the soft robot can move quickly (in cross-gait mode) to the working region and then switch to the single gait mode to perform required tasks such as moving an object.

The foot actuator and body actuator of the soft robots are mold casted using silicone rubber. Each actuator has multiple chambers and multiple actuation channels for propulsion. Due to the complexity of the structures, we have to decompose the structure, and arrange the appropriate casting sequences and bonding interfaces (Figure 1b). The molds for casting are designed based on the structure segmentation and are printed by a high-precision 3D printer. In general, the fabrication of a worm-inspired soft robot can be divided into three steps: the fabrication of REPAs for the feet of the soft robot (step I); the fabrication of the EPA for the main body of the soft robot (step II); and the assembly step for the basic module (step III). The inner and outer molds of the REPAs are separately printed by a 3D printer (I-A) and then assembled together (step I-1). The metal rods ($d = 2$ mm) are inserted to make central channels and pneumatic channels (step I-2, I-B). After that, we pour the mixed silicone rubber (Dragon Skin 30) into the mold for curing (step I-3). The casted silicone rubber is then cured in an oven for 10 h before demolding (I-C).

In our fabrication process, we separately build the two half-parts of EPA and then bond them together to form a whole structure with complex chamber and channel structures. We design the molds for the half structure of EPA and then print it with a 3D printer (II-A). We then assemble the two molds together (step II-1) and insert the metal rods for constructing the channels (II-B). After that, we pour the mixed silicone rubber (Dragon Skin 30) into the mold for curing in an oven (step II-3). After demolding the cured components, the two parts of the actuator can be bonded together with the silicone rubber (II-C). Finally, we assemble the forefoot, main body, and the hindfoot together to form a basic module of the soft robot (III-A).

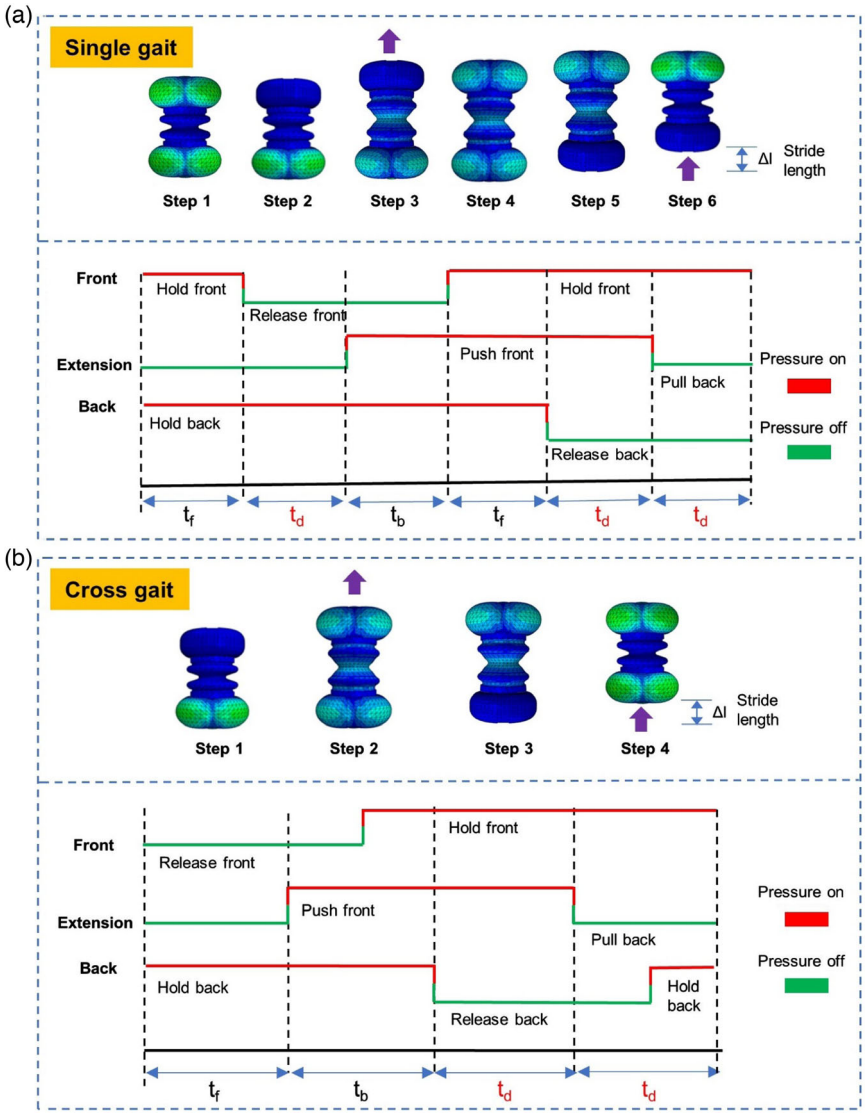

Figure 2. Programmable actuation of the soft actuators for propulsion of the soft robot. a) Single gait mode: single gait mode involves six steps in a complete motion cycle in which the feet and the body are actuated alternatively. b) Cross-gait mode: one cross-gait cycle includes four steps in which the inflation or deflation of the feet actuators synchronize with the elongation of the body actuator.

2.2. Characterization and Evaluation of the Basic Modules

The soft actuators determine the performance of the soft robots in loading capacity and moving speed. The axial elongation of the body actuator affects the stride length and speed of the soft robot, while the radial expansion of the feet actuator determines its suitability for the diameter/size of the pipelines. Moreover, the load capacity is controlled by the output force of the actuators under the inflation states. Thus, we test the mechanical performances of the soft actuators in detail (Figure S1, Supporting Information). In our experimental setup, the deformation of the EPA and REPA is measured by a Magnetostrictive Displacement Sensor (MDS, SDMSA-1000-V11P-MEDS-2XX1). The actuator is installed between two magnetic rings of the MDS, with one end fixed and the other end contacted a magnetic ring. When an air pressure is applied, the EPA/REPA actuator can push the magnetic ring to move so as to generate a displacement (i.e., the deformation of the actuator) due to the elongation or radial expansion.

Figure S1b, Supporting Information, shows that the elongation of the EPA has a linear relation with the applied air pressure under an air pressure of less than 60 kPa and becomes more nonlinear when subjected to a higher air pressure (60–100 kPa). This is mainly because that the chamber volume of the actuator varies nonlinearly with the applied air pressure and that the silicone elastomer has a nonlinear mechanical property under large deformations. The elongation of the EPA, i.e., the maximum displacement of the soft robot in one motion cycle, varies from 0 to 25 mm. It is noted that the EPA in one single module or a serially connected configuration shows little difference in elongation, under the same actuation pressures in the measured range.

The four connected chambers in the REPA are controlled by a same pneumatic channel and can uniformly expand when applying a pneumatic pressure. As shown in Figure S1c, Supporting Information, the maximum expansion is 15 mm under air pressure of 100 kPa (a safe working pressure for actuator). This indicates that the soft tubular robot can be used for pipelines with diameter range of 50–65 mm, although the applied pressure may be adjusted accordingly.

Figure S1d, Supporting Information, shows the experimental platform for measuring the output forces of the soft actuators. In our testing, one end of the EPA is clamped and the other end contacts a six-axis force sensor (SRI-V-171 120-A M3703B SN2704). Figure S1e, Supporting Information, shows the output force generated by the EPA nonlinearly increases with the applied air pressure. The maximum output force can reach up to 160 N under a pressure of 200 kPa. The output force generated by the EPA in one soft robot module and a connected soft robot is almost the same. To measure the output force of the REPA, we put the actuator into a pipe with a diameter of 50 mm, and the pipe is equally cut into four shells, corresponding to one chamber of the actuator. Four micropressure sensors (XJH-100) are fixed on the outside surface of the pipe shell, and the probe of each pressure sensor is perpendicular to the corresponding outer wall of the pipe shell. When an air pressure is applied, the REPA expands radially and pushes the four pipe shells to contact the force sensors. When the air pressure is 250 kPa, the radial output force reaches up to 240 N, which is large enough to support the robot to move vertically. Figure S1f, Supporting Information, shows the relationship between the radial output force and the applied air pressure. The radial output force increases dramatically when the air pressure is larger than 180 kPa because of the larger contact area between the actuator and the pipe shell. Theoretical analysis of the radial expansion and axial elongation of the soft actuators are given in Supporting Information.[17,18]

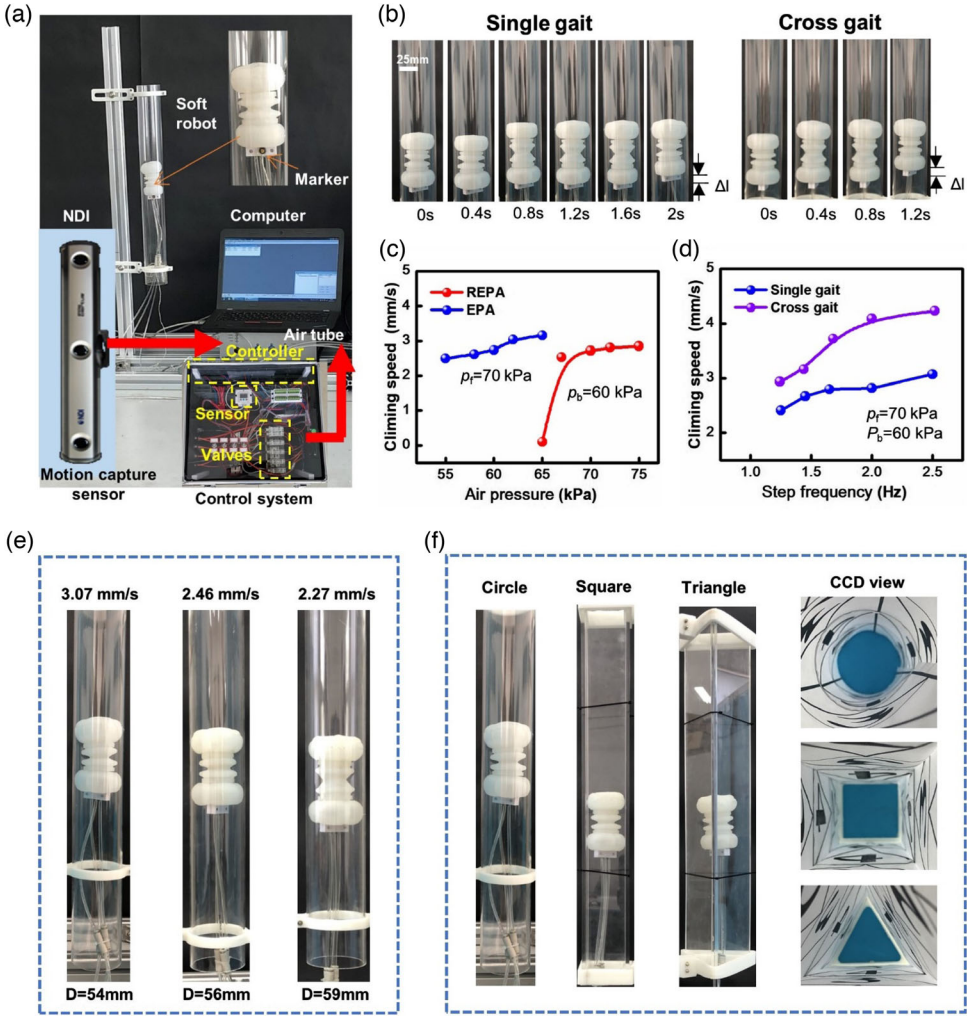

Figure 3. Performance evaluation of the worm-inspired soft robot in a stragight pipe. a) Experimental setup for evaluating the motion performance of the soft robot. b) Photo images of the soft robot in the vertically aligned pipes at different time points using single gait mode and cross-gait mode. c) The relationship between the crawling speed of the soft robot with applied air pressure. d) The relationship between the crawling speed of the soft robot with step frequency. e) The soft robot crawls in a pipe with varying diameter by adjusting the expansion of the REPA to adapt the changing diameter. f) The soft robot can crawl in a pipe with different cross-sectional shapes (e.g., circle, square, and triangle).

The kinematic performance of the worm-inspired soft robot is measured with a 3D motion capture system (**Figure 3**a). The basic module of the soft robot is placed into a vertical pipe and marked on its end. The position of the marker can be tracked by the motion capture sensor (NDI Optotrak) to obtain the moving displacement of the soft robot in the pipe. We build an air

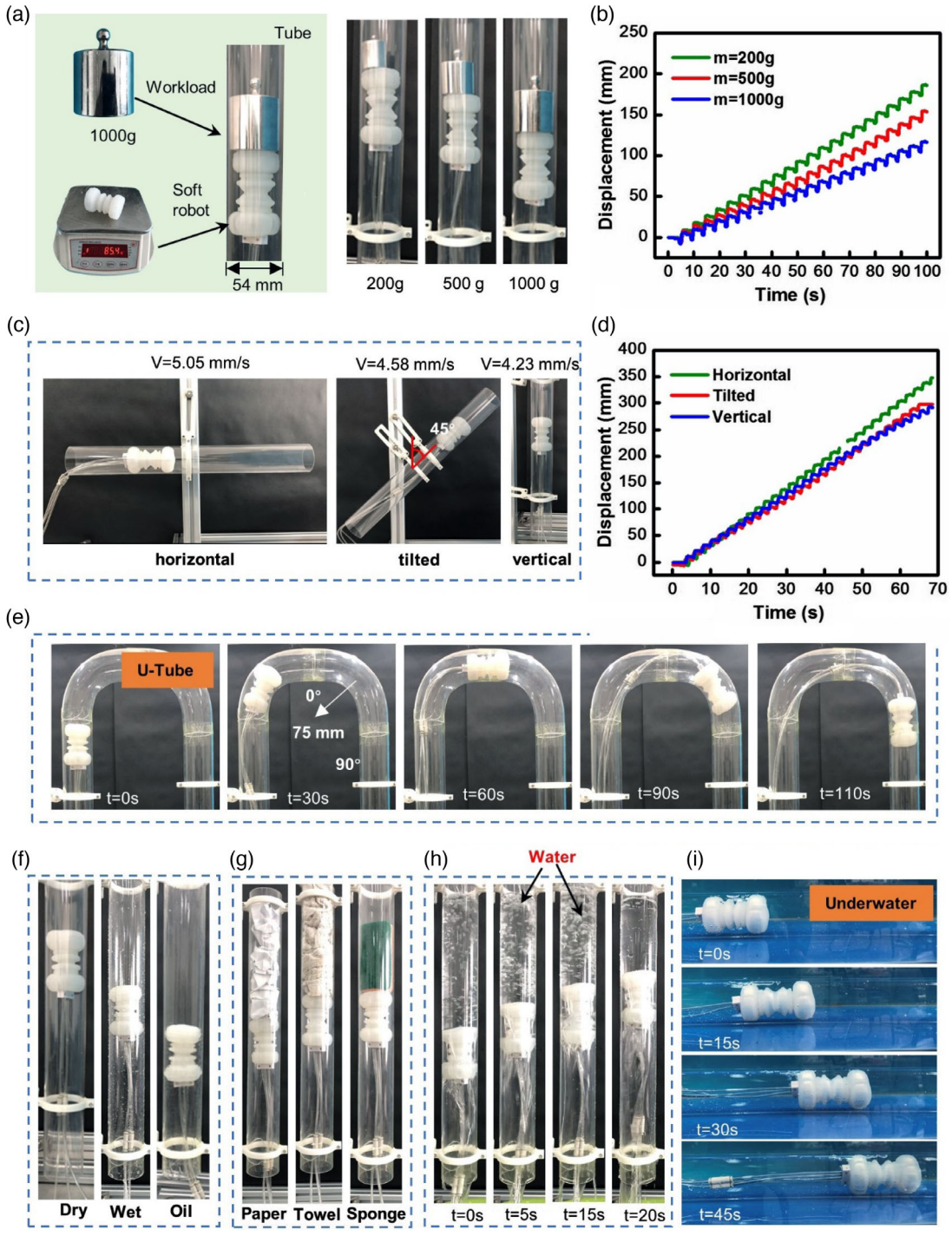

Figure 4. Demonstration of the soft robot under more complex working conditions. a) The soft robot carries a workload that is much heavier than its own weight moves in a vertical pipe. b) Comparison of the kinematic performance of the soft robot with different workloads. c) The soft robot can crawl in a pipe with different title angles (horizontal, tilted, and vertical). d) Kinematic performance of the soft robot in pipes with different title angles. e) The soft robot moves in a "U" shaped pipe and the turning radius is 75 mm. Demonstrations of the soft robot in different working conditions: f) the soft robot moves in a dry, wet and oil pipe; g) it performs a clearing task with paper, towel or sponge in the pipe; h) the soft robot moves vertically with the water column pouring; i) the robot moves when immersed in water.

pressure control system to study the relationship between the moving speed of the robot under different air pressures and switching frequencies. Figure 3b shows the displacement of the soft robot in one motion cycle using the single gait and the cross-gait, respectively (Video S1, Supporting Information). The speed of the soft robot shows a nearly linear relationship with the applied air pressure in EPA (Figure 3c) when the REPA is fixed at a certain air pressure of $p_f = 70$ kPa. However, when the air pressure in the EPA is set at $p_b = 60$ kPa, the soft robot fails to move in a pipe when the air pressure of the feet actuator is less than 65 kPa. The feet actuator only affects the friction between the inner wall of the pipe and the soft robot, and the speed of soft robot is mainly determined by the air pressure of the EPA. It is found that the air pressure of feet actuator (when $p_f > 65$ kPa) has little effect on the moving speed of the soft robot. Figure 3d shows the relationship between the moving speed and the step frequency, in which the moving speed increases with the frequency. It should be noted that the moving speed of a soft robot in cross-gait mode is significantly higher than that in single gait mode at the same step frequency. If the soft robot adopts the single gait to move, and Δl is the stride length of one motion cycle, then the speed of robot can be expressed as $v = \frac{\Delta L}{T} = \frac{\Delta L}{\sum_{i=1}^{6} \frac{1}{f_i}}$, where T is the period of single gait and f_i is the step frequency.

2.3. Demonstration of the Worm-Inspired Soft Robot

The soft robot has good flexibility and adaptability to accommodate a variety of working environment conditions. For example, it can crawl in the pipes with different diameters and different cross-sectional shapes. Figure 3e shows the soft robot crawls in a pipe with varying diameters thorough adjusting the expansion of the REPA to adapt the pipe diameter. It is observed that the increase in the inner diameter of the pipe will lead to an insufficient contact of the feet REPAs with the inner wall of the pipe after air inflation, thereby possible slippage in the crawling and reduction of the motion speed. Under the same actuation frequency, the crawling speed of the soft robot in a pipe of 54 mm diameter can reach to 3.07 mm s^{-1}, but decreases to 2.27 mm s^{-1} as the inner diameter of the pipe increases from 54 to 59 mm (Video S2, Supporting Information). In addition, the soft robot can continuously crawl in a varying diameter pipeline which is further proved the adaptability of the soft robot. As shown in Figure S2 and Video S3, Supporting Information, the soft robot crawls through a smaller diameter pipe ($\phi = 54$ mm) and then moves smoothly into a pipe of a larger diameter ($\phi = 59$ mm). Figure 3f and Video S4, Supporting Information, demonstrate that the annular feet of the soft robot can accommodate different cross-sectional shapes of the pipes such as circular shape, square shape, or triangular shape (Video S5, Supporting Information).

Figure 4a shows the soft robot carrying a workload moves forward in a plexiglass pipe with the diameter of 54 mm. It can be seen that the soft robot can move a weight load (1000 g) of 11 times larger than its own weight (85.4 g) forward in a vertically placed pipe. Video S6, Supporting Information, demonstrates the moving process in experiments, in which the applied air pressure in the feet actuator is 85 kPa and the pressure applied on the body actuator is 60 kPa; the frequency of air pressure switching is 1.25 Hz. Figure 4b shows the motion speed of the soft robot with different workloads. It can be seen that the motion speed of the soft robot decreases with the increase in the workload. Figure 4c and Video S7, Supporting Information, show the soft robot climb in a pipeline with different title angles from 0 to 90°. The speed of the soft robot in a horizontal, tilted, and vertical pipe is 5.05, 4.58, and 4.23 mm s^{-1}, respectively. With the increase in pipe inclination, the moving speed slows down because of the gravity (Figure 4d). Figure 4e and Video S8, Supporting Information, demonstrate the robustness of the soft robot in a U-shaped pipe, where it can turn the corners and crawls back and forth freely. The soft robot can also move in a tube with liquid filled, or oil conditioned, or underwater conditions. Figure 4f and Video S9, Supporting Information, demonstrate the excellent performance of the soft robots in such demanding environments. The soft robot can move in a dry, wet, and oil-covered pipe. Compared with the case in a dry pipe, the speed of the soft robot in a

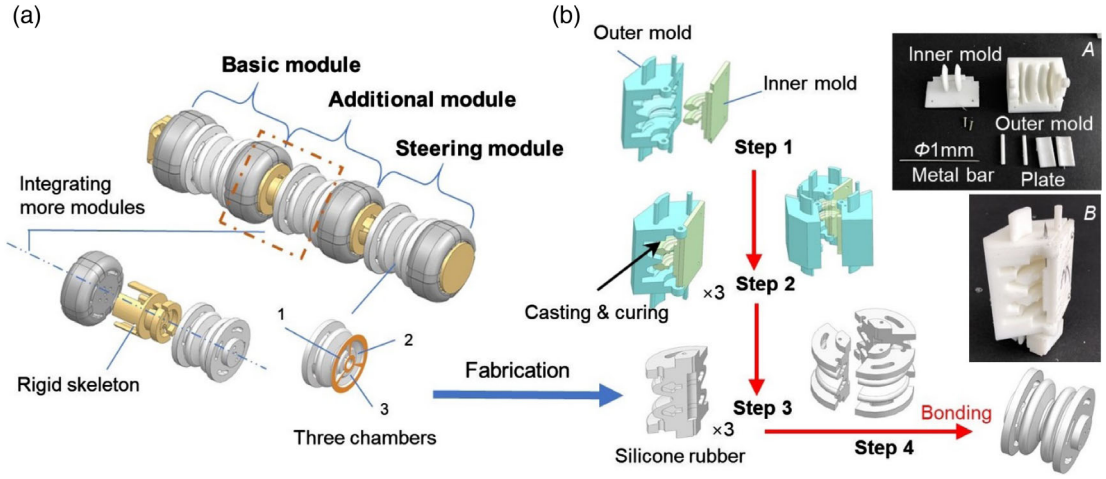

Figure 5. Concept design and fabrication of the soft robot with multiple actuators connected in series. a) Two or more modules could be integrated in series by designed rigid skeletons to form a versatile soft tubular robot. The steering module is designed to adjust moving direction. b) Schematic illustration of the fabrication process of the spatial bending actuator.

Figure 6. Demonstration of the worm-inspired soft robot with multiple actuators under different working conditions. a) Optical images of the soft robot crawling across an obstacle. b) Demonstrations of the steering module bending to arbitrary directions in a 3D space. c) Optical images of the soft robot crawling across an obstacle in "Y"-shaped pipe. d) Optical images of the soft robot crawling across an obstacle in "S"-shaped pipe.

wet and oil-covered pipe is dramatically reduced due to the slippage, especially in the oil-filled pipe; the speed is only ≈1/2 of its speed in a dry pipe. In addition, the soft robot can also perform a clearing task with paper, towel, or sponge in the pipe (Figure 4g and Video S10, Supporting Information). It can move vertically in the pipe with a water column filled, verifying its robust performance in a complicated environment (Figure 4h and Video S11, Supporting Information). The worm-inspired soft robot can move fast underwater because the drainage channels are deployed on its feet, which can significantly reduce the water

resistance in motion (Figure 4i and Video S12, Supporting Information).

3. Soft Robot with Multiple Actuators Connected in Series

To improve the performance of the worm-inspired soft robots, more basic modules of the soft robot can be integrated in series through rigid skeletons (**Figure 5**a). The steering module is designed to change the motion direction in a branched pipeline or pipeline network. The steering module is made of a REPA and a SBPA which has three centrosymmetric chambers that can be actuated independently (Figure 5b). The SBPA can bend in any direction in space by adjusting air pressure in the chambers. The more DOFs and excellent flexibility enable the steering module to be more adaptable and robust. Figure 5b shows the fabrication process of the SBPA. Similarly, the SBPA is divided into three equal parts and each part should be cast-fabricated separately by the 3D printed molds.

The soft robot consisting of more connected modules in series, in particular, with the employment of the steering module, can greatly improve its capability to crawl over obstacles and its flexibility to adjust the heading direction of movement. To valid this advancement, we test the multilegged soft robot using a combined pipe with both straight and elbow segments. In first scenario, two vertically aligned pipes are coaxially arranged (**Figure 6**a), leaving a gap L between them to mimic a potential pipeline fracture gap. The capability of the soft robot to crawl cross the obstacles is demonstrated in Figure 6a and Video S13, Supporting Information. The maximum gap size that the soft robot can cross is expressed as $L_{\max} = h + l + \Delta l_{\max}$, where h is the height of REPA, l is the active length of EPA, and $\Delta l_{\max}$ is the maximum elongation of the EPA. The maximum gap is nearly 0.4 body length, which is superior to other crawling robots in the literature.[16] When the head of the soft robot moves to the position where the pipe breaks, the hindfoot is first actuated to stick on the inner wall of the pipe below, then the body of the soft robot elongates to push the steering module into the pipe above; and the forefoot is then actuated to tightly adhere on the inner wall of the upper section of the pipe, and the body retracts to pull hindfoot forward. Finally, all parts of the soft robot pass through the pipeline gap in a proper order.

The steering module has more DOFs and better flexibility so that it can bend to an arbitrary direction in a 3D space by adjusting the air pressure of the three independent chambers (Figure 6b). The bending direction angle γ can be expressed as $\gamma = \arctan\frac{2p_1 - p_2 - p_3}{\sqrt{3}(p_2 - p_3)}$,[17] where p_1, p_2, and p_3 are the air pressures in the three different chambers, respectively. Figure S3a, Supporting Information, shows the experimental images of the bending profiles of the SPBA under different air pressure from 0 to 140 kPa. Figure S3b, Supporting Information, shows the bending angles of the SPBA when one or two chambers are actuated with air pressure. It indicates that the bending angle has a nearly linear relationship with the applied pressure, and the bending angle actuated by two chambers is slightly larger than that by actuating single chamber. The bending angle (θ) can reach up to 25° when one chamber is actuated with a pressure of $p = 150$ kPa. Figure 6c and Video S14, Supporting Information, demonstrate that the steering module of soft robot can easily adjust the spatial movement direction to cross through the complicated "Y"-shaped pipeline, which has a gap and an angle between the two straight pipelines. Figure 6d and Video S15, Supporting Information, illustrate that soft robot can crawl smoothly in a "S"-shaped pipe by adopting the appropriate control strategy. To further enhance the functionality of the soft robot, a visualization unit is mounted on the head of the soft robot to observe the inside of the pipeline for inspection or navigation purpose, and the robot can then follow the instructions to conduct the needed operations. The visualization unit is powered by a battery and the data are wirelessly transmitted via Bluetooth. **Figure 7** and Video S16, Supporting Information, show that soft robot crawls in a multibranched pipe and the visualization unit constantly captures the internal view of the pipe. When passing through the intersection, the soft robot follows the instruction of control system and turns to B-branch owing to the flexibility of the steering module. We also compare the performance of the soft robots with and without the steering mechanism under same working conditions (Figure S4 and Video S17, Supporting Information). Although the steering strategy can help navigate in the pipe network, there is no significant difference in speed between these two robots. With these robust soft tubular robots, we can perform a variety of tasks such as inspection, cleaning, and maintenance operations through integrated sensors, CCD cameras, or manipulators on the soft robot.[18,19]

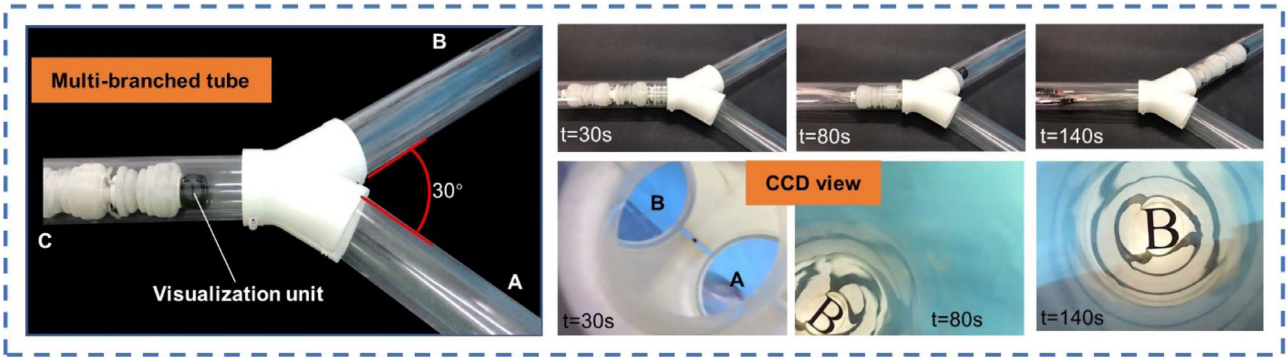

Figure 7. Demonstration of the worm-inspired soft robot with multiple actuators for inspection in a multibranched pipe. The visualization unit is installed on the head of the soft robot. The soft robot can turn to a desired branch according to the observation and real conditions inside of the pipe.

4. Conclusion

In summary, we have developed a novel worm-inspired soft robot capable of traveling through a variety of complicated pipeline or pipeline networks. The soft robot was designed based on soft pneumatic actuation in a modular approach and was easily assembled into a more complex soft robots with multiple legs/modules for practical use. We examined the mechanical performance of soft actuators and verified its performance through systematic experiments. The soft robot can move a load of 11 times larger than its own weight in a vertical pipe. The soft REPA can generate large deformations and enable it to accommodate different sizes and shapes of pipes. It can be used for pipeline inspection without damaging the tube, and it is compatible with challenging surface conditions such as wet or oil-covered surfaces, even underwater. In addition, the steering module for soft robots enables it to bend to an arbitrary direction in a 3D space, leading to excellent flexibility and adaptability so that the soft robot can move in a multibranched pipeline smoothly. Equipped with a visualization unit, the soft robot can perform inspections and navigation in a multibranched pipeline. However, it should be pointed out that the tethered actuation approach for this soft robot may limit its practical application in many scenarios. Thus, an untethered design will be necessary by using an in-house developed micropump and onboard control circuits to make the soft robot free of the external wires and power source in the future. It is expected that the tubular soft robot will provide a useful tool for the inspection, cleaning, and maintenance of pipelines and tunnels.

Supporting Information

Supporting Information is available from the Wiley Online Library or from the author.

Acknowledgements

X.L. and Y.Z. acknowledge the support from Science and Technology Project of Department of Education of Jilin Province, China (grant nos. JJKH20190640KJ and JJKH20200038KJ). X.L. also thanks the support from China Scholarship Council (grant no. CSC201802325005). C.C. acknowledges the financial support from NSF (grant no. ECCS-2024649) and Michigan State University.

Conflict of Interest

The authors declare no conflict of interest.

Data Availability Statement

Research data are not shared.

Keywords

adaptable designs, bioinspired robotics, soft pneumatic actuators, soft robots, tubular robots, worm-inspired robots

Received: June 26, 2021
Revised: August 3, 2021
Published online:

[1] a) P. Chattopadhyay, S. Ghoshal, A. Majumder, H. Dikshit, *J. Eng. Sci. Technol. Rev.* **2018**, *11*, 154; b) R. F. Shepherd, F. Ilievski, W. Choi, S. A. Morin, A. A. Stokes, A. D. Mazzeo, X. Chen, M. Wang, G. M. Whitesides, *Proc. Natl. Acad. Sci.* **2011**, *108*, 20400; c) J. M. Mirats Tur, W. Garthwaite, *J. Field Rob.* **2010**, *27*, 491; d) S. Nansai, R. Mohan, *Robotics* **2016**, *5*, 14.
[2] B. Zhang, Y. Fan, P. Yang, T. Cao, H. Liao, *Soft Rob.* **2019**, *6*, 399.
[3] a) D. Waleed, S. H. Mustafa, S. Mukhopadhyay, M. F. Abdel-Hafez, M. A. K. Jaradat, K. R. Dias, F. Arif, J. I. Ahmed, *IEEE Sens. J.* **2019**, *19*, 1153; b) D. Rus, M. T. Tolley, *Nature* **2015**, *521*, 467.
[4] a) C. Laschi, B. Mazzolai, M. Cianchetti, *Sci. Rob.* **2016**, *1*, eaah3690; b) S. Kim, C. Laschi, B. Trimmer, *Trends Biotechnol.* **2013**, *31*, 287.
[5] a) S. Chen, Y. Cao, M. Sarparast, H. Yuan, L. Dong, X. Tan, C. Cao, *Adv. Mater. Technol.* **2020**, *5*, 1900837; b) S. Chen, Y. Pang, H. Yuan, X. Tan, C. Cao, *Adv. Mater. Technol.* **2020**, *5*, 1901075; c) X. Liu, Y. Zhao, D. Geng, S. Chen, X. Tan, C. Cao, *Soft Rob.* **2020**, *8*, 175; d) S. Chen, Y. Pang, Y. Cao, X. Tan, C. Cao, *Adv. Mater. Technol.* **2021**, *6*, 2100084.
[6] M. T. Tolley, R. F. Shepherd, B. Mosadegh, K. C. Gallow, M. Wehner, M. Karpelson, R. J. Wood, G. M. Whitesides, *Soft Rob.* **2014**, *1*, 213.
[7] a) W. Hu, G. Z. Lum, M. Mastrangeli, M. Sitti, *Nature* **2018**, *554*, 81; b) H. Niu, R. Feng, Y. Xie, B. Jiang, Y. Sheng, Y. Yu, H. Baoyin, X. Zeng, *Soft Rob.* **2020**; c) G. Y. Gu, J. Zhu, L. M. Zhu, X. Zhu, *Bioinspiration Biomimetics* **2017**, *12*, 011003; d) H. T. Lin, G. G. Leisk, B. Trimmer, *Bioinspiration Biomimetics* **2011**, *6*, 026007; e) M. Runciman, J. Avery, M. Zhao, A. Darzi, G. P. Mylonas, *Front. Rob. AI* **2019**, *6*, 141; f) G. Gu, J. Zou, R. Zhao, X. Zhao, X. Zhu, *Sci. Rob.* **2018**, *3*, eaat2874; g) T. Yamamoto, S. Sakama, A. Kamimura, *IEEE Rob. Autom. Lett.* **2020**, *5*, 5034.
[8] C.-Y. Yeh, C.-Y. Chen, J.-Y. Juang, *Extreme Mech. Lett.* **2020**, *39*, 100854.
[9] M. S. Verma, A. Ainla, D. Yang, D. Harburg, G. M. Whitesides, *Soft Rob.* **2018**, *5*, 133.
[10] S. Seok, C. D. Onal, K.-J. Cho, R. J. Wood, D. Rus, S. Kim, *IEEE/ASME Trans. Mechatron.* **2013**, *18*, 1485.
[11] I. Must, F. Kaasik, I. Põldsalu, L. Mihkels, U. Johanson, A. Punning, A. Aabloo, *Adv. Eng. Mater.* **2015**, *17*, 84.
[12] J. Cao, L. Qin, J. Liu, Q. Ren, C. C. Foo, H. Wang, H. P. Lee, J. Zhu, *Extreme Mech. Lett.* **2018**, *21*, 9.
[13] C.-Y. Yeh, S.-C. Chou, H.-W. Huang, H.-C. Yu, J.-Y. Juang, *Extreme Mech. Lett.* **2019**, *26*, 61.
[14] a) T. Wang, L. Ge, G. Gu, *Sens. Actuators, A* **2018**, *271*, 131; b) X. Wang, S. K. Mitchell, E. H. Rumley, P. Rothemund, C. Keplinger, *Adv. Funct. Mater.* **2019**, *30*, 1908821.
[15] Y. Tang, Q. Zhang, G. Lin, J. Yin, *Soft Rob.* **2018**, *5*, 592.
[16] L. Qin, X. Liang, H. Huang, C. K. Chui, R. C.-H. Yeow, J. Zhu, *Soft Rob.* **2019**, *6*, 455.
[17] K. Wakana, H. Namari, M. Konyo, S. Tadokoro, presented at *2013 IEEE Int. Conf. on Robotics and Automation*, IEEE, Piscataway, NJ, **2013**.
[18] L. Wang, Z. Wang, *Soft Rob.* **2020**, *7*, 198.
[19] D. Drotman, S. Jadhav, M. Karimi, P. D. Zonia, M. T. Tolley, presented at *2017 IEEE Int. Conf. on Robotics and Automation (ICRA)*, IEEE, Piscataway, NJ, May–June 2017.